Plant Pathol. J. 32(4) : 300-310 (2016)
http://dx.doi.org/10.5423/PPJ.OA.01.2016.0032
pISSN 1598-2254 eISSN 2093-9280

Research Article Open Access

The Plant Pathology Journal

Visual Analysis for Detection and Quantification of *Pseudomonas cichorii* Disease Severity in Tomato Plants

Dhinesh Kumar Rajendran[1], Eunsoo Park[2], Rajalingam Nagendran[1], Nguyen Bao Hung[1], Byoung-Kwan Cho[2], Kyung-Hwan Kim[3], and Yong Hoon Lee[1,4]*

[1]*Division of Biotechnology, Chonbuk National University, Iksan 54596, Korea*

[2]*Department of Biosystems Machinery Engineering, Chungnam National University, Daejeon 34134, Korea*

[3]*Molecular Breeding Division, National Institute of Agricultural Sciences, Rural Development Administration, Wanju 55365, Korea*

[4]*Advanced Institute of Environment & Bioscience and Plant Medical Research Center, Chonbuk National University, Iksan 54596, Korea*

(Received on January 31, 2016; Revised on February 29, 2016; Accepted on March 13, 2016)

Pathogen infection in plants induces complex responses ranging from gene expression to metabolic processes in infected plants. In spite of many studies on biotic stress-related changes in host plants, little is known about the metabolic and phenotypic responses of the host plants to *Pseudomonas cichorii* infection based on image-based analysis. To investigate alterations in tomato plants according to disease severity, we inoculated plants with different cell densities of *P. cichorii* using dipping and syringe infiltration methods. High-dose inocula (≥ 10^6 cfu/ml) induced evident necrotic lesions within one day that corresponded to bacterial growth in the infected tissues. Among the chlorophyll fluorescence parameters analyzed, changes in quantum yield of PSII (ΦPSII) and non-photochemical quenching (NPQ) preceded the appearance of visible symptoms, but maximum quantum efficiency of PSII (F_v/F_m) was altered well after symptom development. Visible/near infrared and chlorophyll fluorescence hyperspectral images detected changes before symptom appearance at low-density inoculation. The results of this study indicate that the *P. cichorii* infection severity can be detected by chlorophyll fluorescence assay and hyperspectral images prior to the onset of visible symptoms, indicating the feasibility of early detection of diseases. However, to detect disease development by hyperspectral imaging, more detailed protocols and analyses are necessary. Taken together, change in chlorophyll fluorescence is a good parameter for early detection of *P. cichorii* infection in tomato plants. In addition, image-based visualization of infection severity before visual damage appearance will contribute to effective management of plant diseases.

Keywords **:** chlorophyll fluorescence, detection, hyperspectral image, phenome

*Corresponding author.
Phone) +82-63-850-0841, FAX) +82-63-850-0834
E-mail) yonghoonlee@jbnu.ac.kr

Pathogen infection not only affects genomic and metabolic reactions, but also leads to phenotypic changes in host plants. Plant resistance responses against microbial pathogens mainly involve the salicylic acid and jasmonic acid/ethylene-dependent signaling pathways. These regulate gene expression and generate accumulation of pathogenicity-related proteins, phytoalexins and/or other phenolic compounds, which are closely related to secondary metabolism (Dempsey and Klessig, 2012). In addition to disease development and resistance induction, pathogens may lead to changes in carbohydrate metabolism to proliferate in the infected tissues against reorganization of primary metabolism and relocation of metabolites in the host plants (Berger et al., 2007; Bilgin et al., 2010; Ehness et al., 1997).

In view of photosynthetic primary metabolism, light-energy absorbed by chlorophyll is distributed over three

competing processes; it is used in photosynthesis or it is re-emitted as heat or fluorescence (Rodríguez-Moreno et al., 2008). Thus, an increase in chlorophyll fluorescence implies a decrease in photosynthesis and/or heat dissipation (Murchie and Lawson, 2013). Therefore, the sensitivity of photosystem II (PSII) activity has been used to understand the photosynthetic mechanisms as well as the responses of plants to abiotic and biotic stresses (Murchie and Lawson, 2013; Pérez-Bueno et al., 2015; Wagner et al., 2006). Among the chlorophyll fluorescence parameters, the maximum quantum efficiency of PSII (F_v/F_m) and quantum yield of PSII (ΦPSII) in the light-adapted state, and non-photochemical quenching (NPQ) are generally used to quantify the photosynthetic efficiency of plants.

Many pathogens target carbon metabolism or the photosynthetic apparatus and suppress photosynthesis of the infected plants (Berger et al., 2004; Bilgin et al., 2010; Bonfig et al., 2006). Tao et al. (2003) showed that down-regulation of genes encoding photosynthetic functions was detectable earlier with an avirulent (incompatible) strain than with a compatible (virulent) strain during the interaction of *Arabidopsis* with *Pseudomonas syringae*. Zou et al. (2005) observed a decrease in ΦPSII as well as an increase in NPQ in leaf areas infiltrated with avirulent *P. syringae* pv. *glycinea*, although little effect was observed during compatible interaction. In contrast, Bonfig et al. (2006) reported that F_v/F_m, ΦPSII, and NPQ decreased earlier in hypersensitive reactions than in compatible interaction when *Arabidopsis* was infected with *P. syringae* pv. *tomato* DC3000 (Pst DC3000), and the changes were restricted to the vicinity of the infection site. Rodríguez-Moreno et al. (2008) observed that NPQ initially increases during *P. syringae* pv. *phaseolicola* (compatible) or Pst DC3000 (incompatible) infection on bean plants, but then is decreases at the later stages of infection. By compiling evidence from previous reports, Rojas et al. (2014) argued that upregulation of primary metabolism modulates signal transduction cascades that lead to plant defense responses.

A reliable, sensitive, and selective method for detecting and monitoring plant diseases is essential in the reduction of economic losses by diseases and the environmental impacts of fungicide use. Symptoms result from alteration of the infected tissues, and chlorosis has been identified as the main cause of reduced photosynthesis (Bilgin et al., 2010; Ehness et al., 1997; Kolber et al., 2005). Because of the changes in metabolism underlying symptom development, various spectroscopic and imaging techniques have facilitated the detection of plant diseases (Belin et al., 2013; Furbank and Tester, 2011; Wang et al., 2013). Among them, chlorophyll fluorescence analysis techniques have been used for presymptomatic stress detection and can be used at lab to field scales, as well as in remote sensing (Berger et al., 2007; Chaerle et al., 2004; Murchie and Lawson, 2013; Pineda et al., 2011; Rodríguez-Moreno et al., 2008).

To the best of our knowledge, no study has reported the metabolic and phenotypic responses of host plants based on *P. cichorii* infection severity. Therefore, in this study, to investigate changes in host plants based on infection progression, we used tomato plants as model host and inoculated with different cell densities of *P. cichorii* by dipping leaves into bacterial suspensions, which mimics the natural infection process, and by syringe infiltration. After infection, we analyzed the development of symptoms and bacterial growth within the infected leaf tissues and evaluated the influence of disease severity on various parameters of chlorophyll fluorescence. Furthermore, visible/near infrared (VIS/NIR) and chlorophyll fluorescence hyperspectral images were analyzed to determine and distinguish the degree of infection.

Materials and Methods

Bacterial strain and inoculum preparation. *P. cichorii* JBC1 (Yu and Lee, 2012) was revived from glycerol stock by streaking onto an Luria-Bertani (LB) agar plate and incubated at 25°C as needed. *P. cichorii* JBC1 cells from an overnight cultured LB plate were inoculated in a 50 ml of LB broth containing vancomycin and incubated at 25°C overnight (Nagendran and Lee, 2015). Overnight culture was centrifuged for 10 minutes at 4,000 rpm, and the pellet was washed twice with distilled water (DW) followed by suspension in 10 mM $MgCl_2$ solution. The concentration of the bacterial inoculum was adjusted to OD_{600} = 0.2 (1×10^8 colony forming unit (cfu)/ml) using a spectrophotometer. Cells were diluted 100-fold with 10 mM $MgCl_2$ to low concentrations ($\leq 1 \times 10^8$ cfu/ml) or concentrated by centrifugation to higher concentrations (5×10^8 cfu/ml), and a final concentration of 0.025% Silwet L-77 was added to each bacterial inoculum.

Pathogen inoculation and disease severity assay. To assay disease severity depending on inoculum concentration, 3- to 4-week-old tomato plant seedlings (*Solanum lycopersicum* cv. Seo Gwang) were subjected to infection with *P. cichorii* JBC1 (Hung et al., 2014) by dipping the leaves of each plant into one of the bacterial cell suspensions (1×10^2, 10^4, 10^6, 10^8, and 5×10^8 cfu/ml) prepared as described above. After inoculation, the seedlings were air dried, allowed to grow in high humidity for 12 hours, and then transferred to a growth chamber at 25°C with a 16-hour light/8-hour dark photoperiod, and 65–70% relative humidity. Control plants were treated with 10 mM $MgCl_2$. Disease symptoms of infected leaves were record-

ed 1, 2, and 3 days after inoculation (dai) by measuring percentage of the diseased leaf area using the histogram tool in Photoshop (CS5; Adobe Systems Corporation, San Jose, CA, USA), and disease severity of each treatment was calculated using the following formula: Disease severity (%) = total percentage of diseased leaves/total number of leaves. Five leaves from five individual plants were tested for each treatment, and data were obtained from three independent experiments.

To assay whether the data obtained from dipping inoculation were comparable to those of syringe infiltration method, which enables localization of the inoculated area and symptom development, we infiltrated various cell concentrations (1×10^2, 10^4, 10^6, 10^8, and 5×10^8 cfu/ml) into a half portion of tomato leaves using a needleless syringe. The infiltrated seedlings were exposed to high humidity and maintained in a growth chamber as described above and the leaves were used for chlorophyll fluorescence assay and image analysis.

***In planta* bacterial growth assay.** Infected leaves from each plant were collected with a cork borer, and 1 cm^2 leaf disks were surface-sterilized with 15% H_2O_2 for 3 minutes and washed twice with sterile DW. Tissues were homogenized in 1 ml sterile DW using a mortar and pestle and serially diluted and plated on LB agar media containing vancomycin (Nagendran and Lee, 2015). Bacterial colonies were counted after 24 hours of incubation at 25°C, and quantities of bacteria were calculated as cfu/cm^2. Three leaves were evaluated from each bacterial concentration (1×10^2, 10^4, 10^6, 10^8, and 5×10^8 cfu/ml), and each experiment was repeated at least three times. *In planta* bacterial growth was analyzed 1 and 3 dai.

Chlorophyll fluorescence kinetics. Chlorophyll fluorescence was measured using a portable chlorophyll fluorometer MINI-PAM-II (Walz, Effeltrich, Germany) following the method of Rodríguez-Moreno et al. (2008) with minor modifications. The measuring system possesses a red actinic light (light-emitting diode [LED] emission peak 655 nm) plus far-red light (LED emission peak 740 nm) for fluorescence excitation, actinic illumination, and saturating light pulses. Chlorophyll fluorescence was estimated using a dark leaf clip DLC-8 (8 mm in diameter; Walz) positioned at a right angle with respect to the leaf surface at a distance of 7 mm. The chlorophyll fluorescence of dipping inoculated plants was assessed from randomly selected areas in non-symptomatic leaves or at the edges of symptomatic leaf areas at 1, 2, and 3 dai. Values from syringe infiltrated leaves were also obtained from three areas, the inoculated region, the edge of the water soaked or diseased area, and healthy places, and the values were compared with those from the dipping assay.

Leaves were dark-adapted for 20 minutes before measurement. After dark adaptation, F_v/F_m was measured by subjecting the leaves to a short pulse of 800 μmol m^{-2} s^{-1}, and ΦPSII and NPQ were recorded under the presence of actinic light (300 μmol m^{-2} s^{-1}). The readings were noted at regular intervals of 25 seconds to achieve saturation. The final steady state readings were used for analysis and to predict differences in control and infected plants. The values were automatically calculated by the WinControl-3 software (Walz), and all parameters were obtained from attached leaves. Three leaves from three plants per treatment were analyzed, and the experiments were repeated three times with similar results.

Measurement of chlorophyll content. To measure the relative chlorophyll content in infected leaves, leaf tissues (100 mg) were soaked in 1 ml of 80% (v/v) acetone and homogenized using mortar. The homogenized mixture was centrifuged at 5,000 rpm for 10 minutes. The optical density of the supernatant was measured at 663 and 645 nm, and total chlorophyll was determined using the following formula: total chlorophyll = 8.02 OD_{663} + 20.20 OD_{645} (Farissi et al., 2013). Chlorophyll content was also measured using an SPAD-502 meter (Minolta Co., Tokyo, Japan), and both readings were compared. Chlorophyll content was measured 1, 2, and 3 dai from three leaves of three plants per treatment with three independent replications.

VIS/NIR and chlorophyll fluorescence hyperspectral image acquisition. The hyperspectral image system reported by Lee et al. (2014) was used for this study with some modifications. The line scan imaging spectrograph (VIS/NIR Hyperspec; Headwall Photonics, Fitchburg, MA, USA) with a spectral range from 400 to 1,000 nm was mounted together with an electron multiplying charge-coupled device (EMCCD) camera (Luca RDL-604M; Andor Technology, South Windsor, CT, USA). The hyperspectral sensor system stood on a manual positioning XY-frame and was illuminated by six 100 W halogen lamps (Model DC-950; Dolan Jenner, Boxborough, MA, USA) with a fiber bundle placed in the inside bottom part of chamber. Imaging data were recorded in a dark chamber to prevent the influence of external illumination and to realize constant measurement conditions. To obtain hyperspectral images, the infected leaves were detached from the plants and fixed horizontally on a black board directly before hyperspectral analysis. The board was placed on a table that was mobilized by a computer-controlled uniaxial motor (0.025 m/sec, XNN10-0180-M02-21; Velmex Inc., Bloomfield, NY, USA). Hyperspectral images were

taken 1, 2, and 3 dai. One to three leaves from each of three plants per treatment were analyzed, and the experiments were repeated at least three times.

Hyperspectral chlorophyll fluorescence images were obtained using the same image system as described above. The illumination system was composed of 4 ultraviolet (UV) LEDs (365 nm). The mounted leaf samples were dark-adapted for 20 minutes before measurements, exposed to UV light for 2 minutes, and the steady-state chlorophyll fluorescence images were captured.

The hyperspectral images from the two cameras were recorded on a personal computer, and MATLAB software (version 7.0.4; Mathworks, Natick, MA, USA) was used to process and analyze hyperspectral images. For each series of measurements, white and dark calibrations were performed to obtain the reflectance R from the raw data. Wavelengths were selected by principal component analysis (PCA) and used for spectroscopy analysis.

Results

Disease severity and symptom development according to infection degree. Infection severity, along with a number of physiological or environmental factors, has been demonstrated to influence the expression of disease symptoms. To regulate infection severity and symptom development, we inoculated tomato plants with different cell densities of *P. cichorii* JBC1. When the leaves of tomato plants were infected with a high dose of cells ($\geq 10^8$ cfu/ml), evident necrotic lesions developed within a day (Fig. 1, Supplementary Fig. 1). Although symptom development was delayed and reduced in comparison with that of high inocula, small necrotic spots were also observed with 10^6 cfu/ml inoculation by 1 dai. At 3 dai, disease severity was 1.5%, 11.0%, and 17.0% when 10^6, 10^8, and 5×10^8 cfu/ml cells were inoculated, respectively. However, no visible symptoms were observed at either 10^2 or 10^4 cfu/ml inoculation until 3 dai. The highest bacterial dosage (5×10^8 cfu/ml) sometimes induced water-soaked symptoms in whole young leaves after high humidity treatment, and the leaves dried out by 1 dai.

Internal growth of *P. cichorii* in tomato leaves. We further evaluated the *in planta* growth of *P. cichorii* JBC1 by quantifying internal populations in infected leaf tissues. The bacterial cell population was significantly lower by inoculation with 10^6 cfu/ml of cells (1.6×10^3 cfu/cm^2) compared to inoculation with 10^8 cfu/ml (6.8×10^4 cfu/cm^2) at 1 dai (Fig. 2). The difference in internal bacterial populations between high ($\geq 10^8$ cfu/ml) and low ($\leq 10^6$

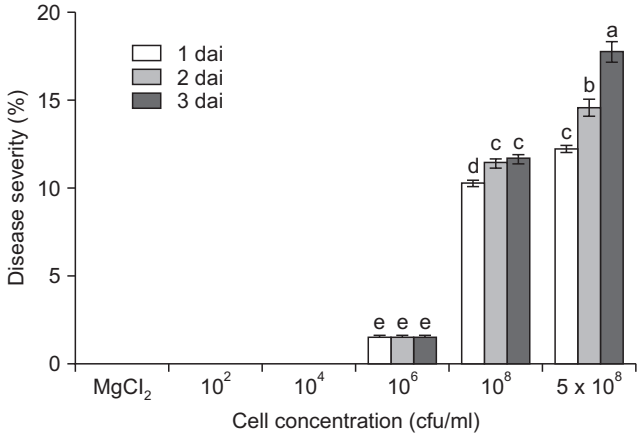

Fig. 1. Disease severity in tomato plants after inoculation with different cell concentration of *Pseudomonas cichorii* JBC1. Leaves of 3- to 4-week-old tomato plants were treated with various cell concentrations (1×10^2, 10^4, 10^6, 10^8, and 5×10^8 cfu/ml) of *P. cichorii* via the dipping method, allowed to grow in high humidity for 12 hours, and incubated in a growth chamber at 25°C with a 16-hour light/8-hour dark photoperiod. Disease severity in infected leaves was measured by direct estimation of the disease area percentage 1, 2, and 3 days after inoculation (dai). The data obtained are the mean ± standard deviation from three independent experiments. Means with the same letter were not significantly different on Tukey's rest ($P \leq 0.05$) run on SAS software.

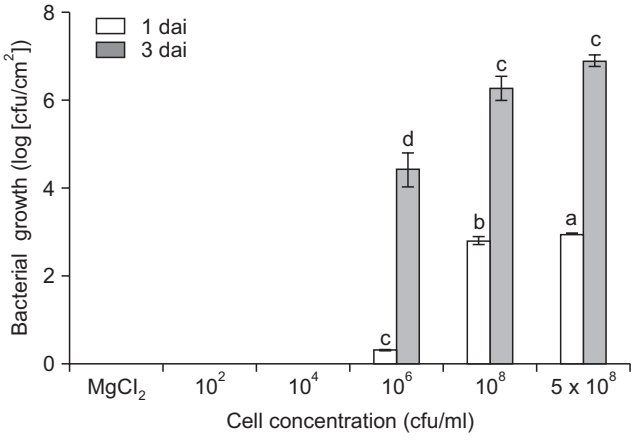

Fig. 2. Assessment of *in planta* population growth of *Pseudomonas cichorii* JBC1. Leaves of 3- to 4-week-old tomato plants were dipped in various bacterial cell concentrations (1×10^2, 10^4, 10^6, 10^8, and 5×10^8 cfu/ml), and the infected leaves were collected and homogenized 1 and 3 days after inoculation (dai). Serially diluted samples were plated onto Luria-Bertani agar plates containing vancomycin. After incubation at 25°C for 24 hours, the number of colonies was counted and normalized to the value per cm^2 of sampled leaves. Data are the mean ± standard deviation from three independent biological samples, and values denoted by the same letters are not significantly different at $P \leq 0.05$ according to Tukey's test.

cfu/ml) cell inoculations directly correlated with disease severity in the tomato leaves. No bacterial cells were detected from the leaf samples of ≤ 10^4 cfu/ml inoculation.

Changes in photosynthetic efficiency. Infection of host plants by pathogens leads not only to the induction of defense reactions but also to changes in carbohydrate metabolism. To investigate the influence of disease severity on photosynthesis levels, changes in photosynthetic activity of tomato plants were assessed after inoculation with different amounts of bacterial cells. While F_v/F_m remained stable in low-dose inoculated leaves (≤ 10^4 cfu/ml), the value progressively and significantly decreased in high-dose inoculated leaves (≥ 10^8 cfu/ml) over the first 3 dai, which correlated to differences in extent of symptom development (Fig. 3A). Even with inoculation of 10^6 cfu/ml cells, the values were slightly decreased, indicating a loss in the efficiency of primary photochemistry related to symptom development, but the photosynthetic efficiency was stably maintained until 3 dai.

We also analyzed ΦPSII at different time points after infection with different cell densities. The changes in ΦPSII were dependent on inoculum densities and occurred earlier and to a greater extent in leaves inoculated with higher concentrations of bacterial cells (Fig. 3B). The value of ΦPSII at low concentrations of inocula (≤ 10^4 cfu/ml) decreased at 2 and 3 dai compared to those of the control. The values were significantly suppressed from 1 dai and decreased to 0.16, 0.09, and 0.06 at 10^6, 10^8, and 5×10^8 cfu/ml, respectively, 3 dai. The results indicated that even low concentrations of inoculation influenced ΦPSII from the initial infection stage. Bacterial infection severely paralyzes photosynthesis of infected plants, and the infection leads to a decline in F_v/F_m, ΦPSII, and NPQ before symptoms are visible with naked eye (Bonfig et al., 2006). In our study, changes in ΦPSII were observed at low concentrations even when the leaves had no visible symptoms, which may help us to detect the presence of pathogens in plants before symptom development.

In general, differences in NPQ values did not correlate with inoculated cell concentrations and symptom development. The NPQ values, which were detectable from 1 dai, slightly increased by inoculation with pathogens (Fig. 3C). At lower bacterial concentrations of 10^2 and 10^4 cfu/ml, the NPQ values increased slightly up to 0.48 and 0.49, respectively, by 3 dai. NPQ values decreased at high concentrations (5×10^8 cfu/ml) of inoculation because of the heavy tissue damage.

Changes in chlorophyll content in pathogen-inoculated leaves. Chlorosis by infection with pathogens has been recognized as a main cause of reduced photosynthesis and

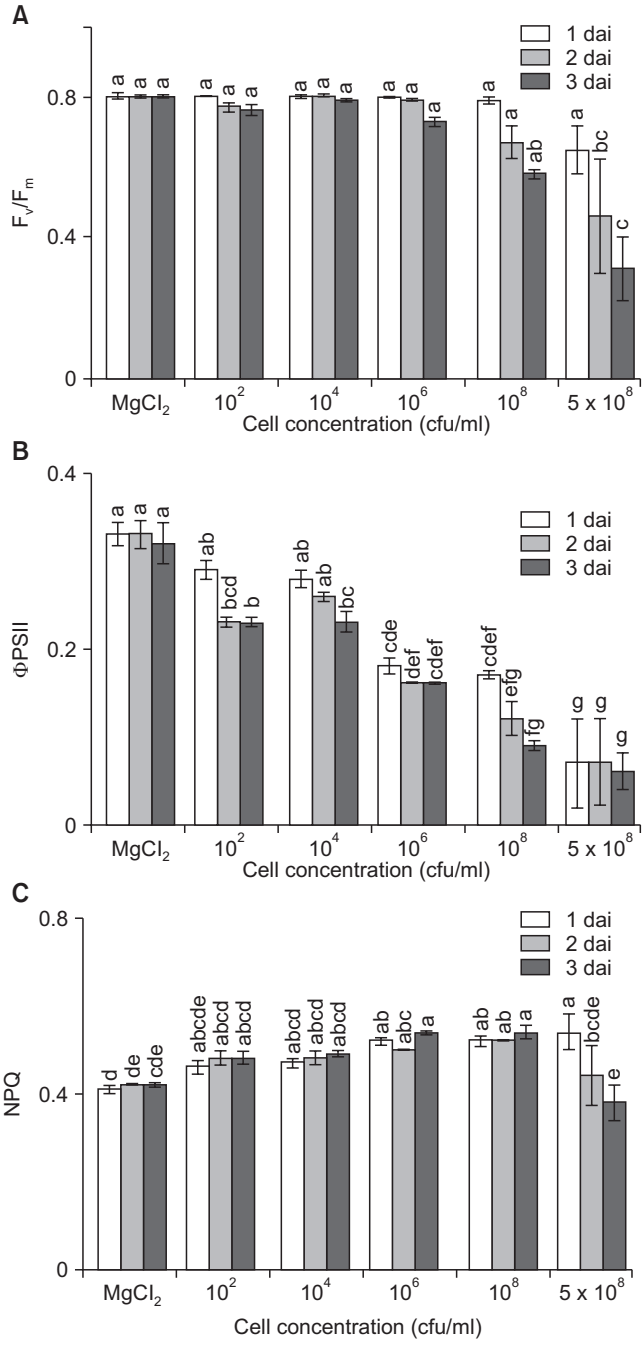

Fig. 3. Time course changes of chlorophyll fluorescence parameters depending on inoculum densities. (A) Maximum quantum efficiency of photosystem II (PSII) (F_v/F_m), (B) effective PSII quantum yield (ΦPSII), and (C) non-photochemical quenching (NPQ) are shown. Leaves of 3- to 4-week-old tomato plants were dipped in various cell concentrations (1×10^2, 10^4, 10^6, 10^8, and 5×10^8 cfu/ml), exposed to high humidity for 12 hours, and incubated in a growth chamber at 25°C with a 16-hour light/8-hour dark photoperiod. The efficiency of excitation capture was recorded after the dark adapted state 1, 2, and 3 days after inoculation (dai). The data obtained represent the mean ± standard deviation from three independent experiments with three replicates. Means with the same letter were not significantly different on Tukey's test ($P \leq 0.05$).

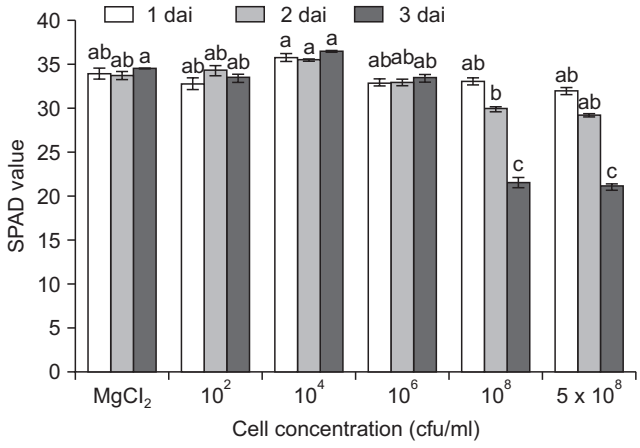

Fig. 4. Changes in chlorophyll content in leaves of tomato plants infected by *Pseudomonas cichorii* JBC1. Leaves of 3- to 4-week-old tomato plants were dipped in various cell concentrations (1×10^2, 10^4, 10^6, 10^8, and 5×10^8 cfu/ml), exposed to high humidity for 12 hours, and incubated in a plant growth room at 25°C with a 16-hour light/8-hour dark photoperiod. The chlorophyll content was measured by SPAD-502 meter at 1, 2, and 3 days after inoculation (dai). The data obtained represent the mean ± standard deviation from three independent experiments with three replicates. Means with the same letter were not significantly different on Tukey's test ($P \leq 0.05$).

decreased yield. To evaluate the direct influence of bacterial infection on chlorophyll, we assayed the time course change in chlorophyll content (Fig. 4). A decrease in chlorophyll content was observed 1 dai only when plants were inoculated with high inoculum densities ($\geq 10^8$ cfu/ml), and the content went down significantly up until 3 dai, indicating the collapse of chlorophyll.

VIS/NIR hyperspectral images. Necrotic or chlorotic lesions caused by pathogen infection influence the reflectance of infected tissues. In this study, among visible and infrared spectra, wavebands from 478 to 683 nm were the most effective for detecting non- or pre-symptomatic infection, which were identified using PCA-based statistical methods. The VIS/NIR hyperspectral images obtained from syringe-infiltrated leaves 1 dai allowed for differentiation between infected and non-infected areas of *P. cichorii*-inoculated tomato leaves (Fig. 5). In general, the VIS/NIR spectra of infected areas shifted from yellow into red according to the necrotic severity. Although there were no visible symptoms in the control leaves, non-symptomatic changes were clearly detected in the VIS/NIR images at low inocula ($\leq 10^4$ cfu/ml) 3 dai. In addition, although the hyperspectral images discerned symptomatic from pre-symptomatic tissue areas, the physical damages were not clearly differentiated from pathogenic necrosis or infection.

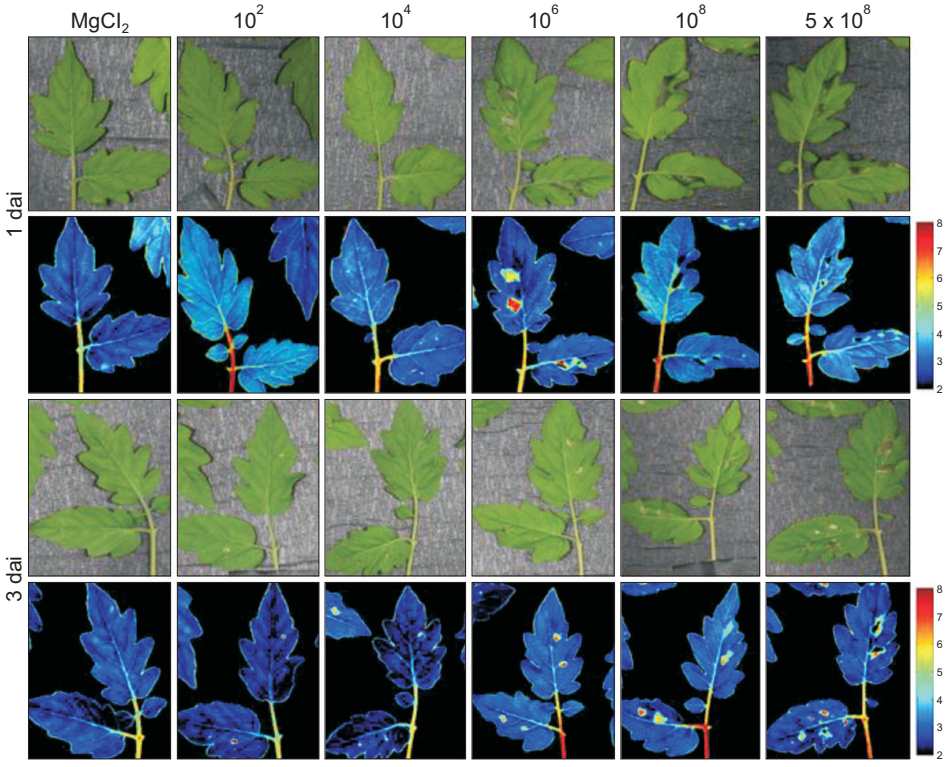

Fig. 5. Visible and near infrared hyperspectral images of tomato leaves infected with *Pseudomonas cichorii* JBC1. Leaves of 3- to 4-week-old tomato plants were infiltrated with various cell concentrations (1×10^2, 10^4, 10^6, 10^8, and 5×10^8 cfu/ml) of *P. cichorii* using a needleless syringe, exposed to high humidity for 12 hours, and incubated in a growth chamber at 25°C with a 16-hour light/8-hour dark photoperiod. Images were obtained 1 and 3 days after inoculation (dai). Images of the fluorescence parameters are displayed with the help of a false color code ranging from 2.0 (black) to 8.0 (purple). Representative measurements are shown here.

Based on the changes in parameters from the syringe infiltration assay, leaves inoculated by the dipping method were also investigated. The images obtained of leaves inoculated with 10^2 cfu/ml of *P. cichorii* by the dipping method showed no difference from the $MgCl_2$-inoculated control (Fig. 6). However, plants inoculated with 10^4 cfu/ml by the same method showed yellow spots in hyperspectral images compared to the uninoculated control 1

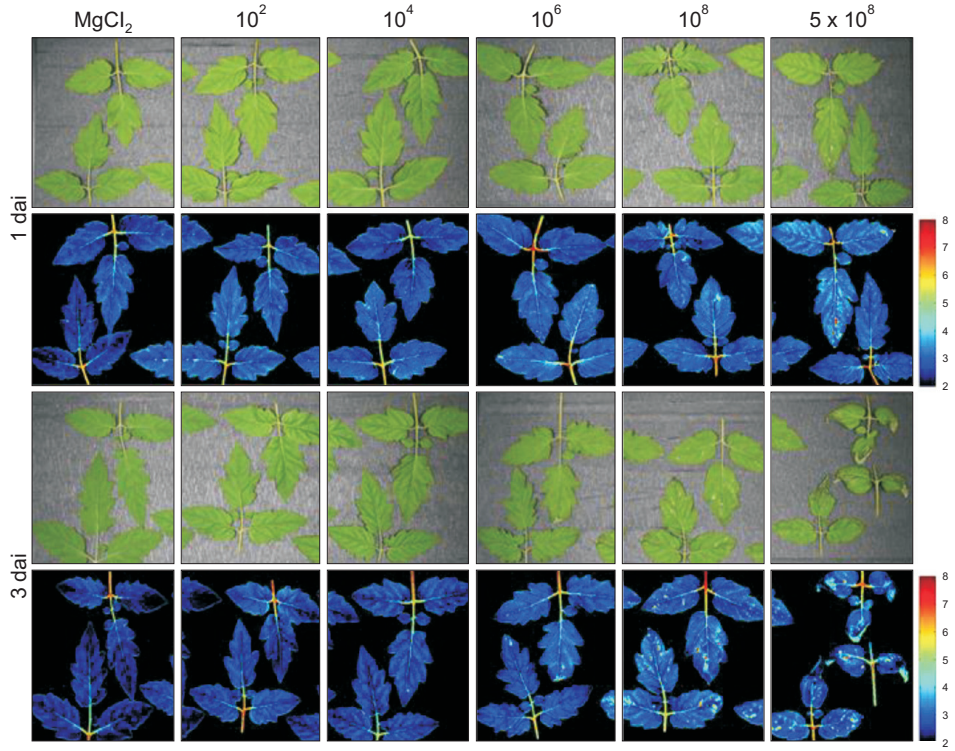

Fig. 6. Visible and near infrared hyperspectral images of tomato leaves infected with *Pseudomonas cichorii* JBC1. Leaves of 3- to 4-week-old tomato plants were dipped in various cell concentrations (1×10^2, 10^4, 10^6, 10^8, and 5×10^8 cfu/ml) of *P. cichorii*, exposed to high humidity for 12 hours, and incubated in a growth chamber at 25°C with a 16-hour light/8-hour dark photoperiod. Images were obtained 1 and 3 days after inoculation (dai). Images of the fluorescence parameters are displayed with the help of a false color code ranging from 2.0 (black) to 8.0 (purple). Representative measurements are shown here.

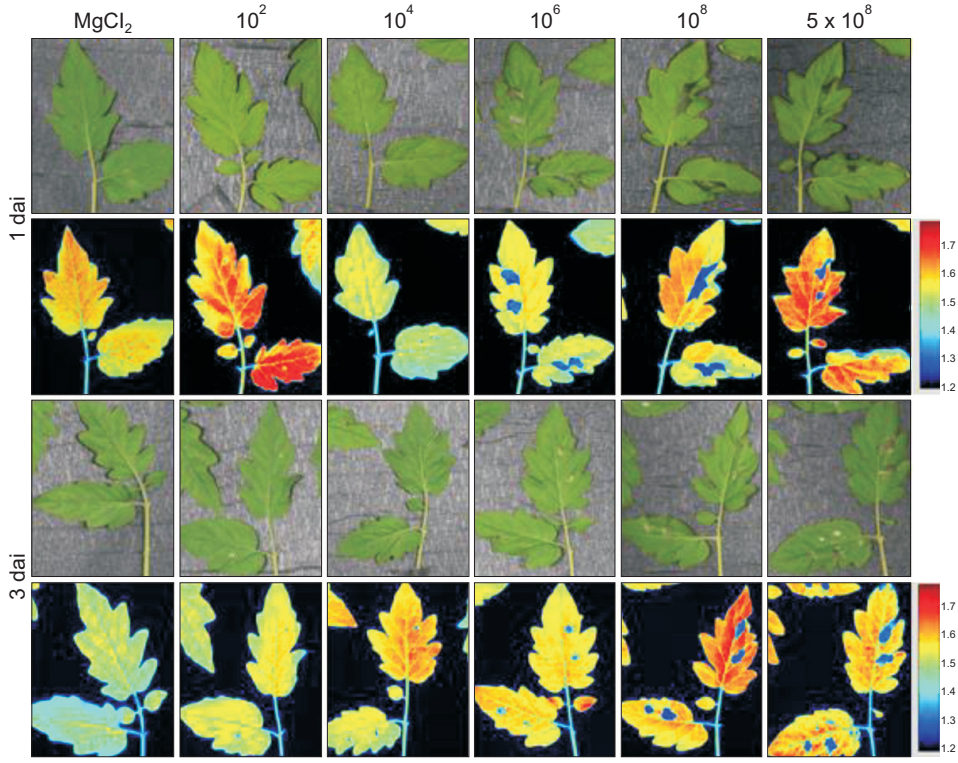

Fig. 7. Chlorophyll fluorescence images of tomato leaves inoculated with different densities of *Pseudomonas cichorii* JBC1 cells. Leaves of 3- to 4-week-old tomato plants were infiltrated with various cell concentrations (1×10^2, 10^4, 10^6, 10^8, and 5×10^8 cfu/ml) of *P. cichorii* using a needleless syringe, exposed to high humidity for 12 hours, and incubated in a growth chamber at 25°C with a 16-hour light/8-hour dark photoperiod. The images were obtained 1 and 3 days after inoculation (dai). Images of fluorescence parameters are displayed with the help of a false color code ranging from 1.2 (black) to 1.9 (purple). Representative measurements are shown here.

dai, and the color weakened by 3 dai, indicating invisible influence in the initial 10^4 cfu/ml inoculation. The VIS/NIR images from leaves inoculated with 10^6 cfu/ml also showed clear differentiation between infected areas 1 dai despite lack of visible symptoms, which suggests pre-symptomatic detection of infection. The infected areas, which showed no visible symptoms or symptomatic areas, were also distinguished by hyperspectral images with a 10^8 cfu/ml inoculum 1 and 3 dai. In addition, since shifts in the spectrum occurred locally at the infection site and in the tissues immediately surrounding the sites, these results indicate that pre-symptomatic infections can also be visualized using a VIS/NIR hyperspectral imaging system.

Chlorophyll fluorescence hyperspectral images. Infection by pathogen influences reflectance of chlorophyll fluorescence, which causes a change in the spectrum. In this study, chlorophyll fluorescence images of areas infected by syringe infiltration shifted into blue (Fig. 7). Although leaves inoculated with $\leq 10^4$ cfu/ml did not show visible symptoms 1 and 3 dai, changes in the chlorophyll fluorescence images were observable compared to the control ($MgCl_2$), indicating an invisible interaction at 10^4 cfu/ml inoculation. The images obtained from a high-density inoculation ($\geq 10^6$ cfu/ml) clearly showed differentiable blue spots in the infected areas. Although the differences between symptomatic areas and pre-symptomatic areas (nearby) were not visibly discernible, the hyperspectral images were able to identify differences and showed blurry blue spots in the pre-symptomatic areas.

The images obtained from the leaves infected by dipping inoculation did not show differentiation between infected and non-infected areas (Supplementary Fig. 2). Because the changes in color in the *P. cichorii* inoculated leaves were not detectable after $MgCl_2$ infiltration, they were presumably due to the pathogen infection, but further studies are needed to corroborate this evidence.

Discussion

Pathogen infection influences metabolic and phenotypic reactions, as well as genomic responses in plants. In this study, to understand the photosynthetic responses of host plants to infection severity by bacterial pathogens, we inoculated different cell densities of *P. cichorii* into tomato plants by dipping and syringe infiltration methods. Necrotic symptoms developed within a day when the leaves of tomato plants were infected with high doses of bacterial cells ($\geq 10^6$ cfu/ml), while no visible symptoms were observed at $\leq 10^4$ cfu/ml inoculation until 3 dai (Fig. 1, Supplementary Fig. 1). In a previous study by Looseley and Newton (2014), variations in the degree of symptom expression were caused by differences in levels of infection and plant genotype. Flood inoculation of tomato seedlings with $OD_{600} = 1$ ($2–5 \times 10^8$ cfu/ml) of Pst DC3000 caused severe necrotic symptoms within 1 dai, but seedlings inoculated with $OD_{600} = 0.1$ ($2–5 \times 10^7$ cfu/ml) exhibited discrete necrotic lesions 3 dai (Uppalapati et al., 2008). Disease in wheat and coriander inoculated with *Xanthomonas translucens* pv. *translucens* and *P. syringae* pv. *coriandricola*, respectively, also developed faster and more severely at higher ($> 10^7$ cfu/ml) inocula (Refshauge et al., 2010; Stromberg et al., 1999).

Symptom development in tomato plants depending on *P. cichorii* inoculum concentration corresponded to bacterial cell growth in the infected tissues, which showed similar results to previous studies (Rodríguez-Moreno et al., 2008; Stromberg et al., 1999; Uppalapati et al., 2008). Pauwelyn et al. (2011) reported that single sprinkler irrigation with water containing 10^2 cfu/ml of *P. cichorii* was sufficient to cause midrib rot in butterhead lettuce, and significantly higher disease was caused at 10^6 cfu/ml inoculation. In spite of no disease even at 10^4 cfu/ml inoculation in our study, development of symptoms by 10^2 cfu/ml of *P. cichorii* on butterhead lettuce due to differences in the inoculum quantity and condensation of inocula between the lettuce leaves related to overhead sprinkler usage and because of differences in the environment. In our study, we also sometimes observed necrosis of leaf edges with $\leq 10^4$ cfu/ml of dipping inoculation with *P. cichorii*, indicating condensation of inocula in water droplets formed at the edges of the leaves.

In most previous reports, because of technical difficulties in differentiating between infected and uninfected areas, the influences of pathogen infection on chlorophyll fluorescence was studied using syringe infiltration methods (Bonfig et al., 2006; Rodríguez-Moreno et al., 2008). In this study, to understand the influence of infection severity on chlorophyll fluorescence based on the observations from syringe infiltration assay, tomato leaves infected with *P. cichorii* by dipping methods were assayed to mimic a natural infection rather than an apoplastic inoculation. F_v/F_m and ΦPSII were significantly decreased in high-dose inoculated tomato leaves ($\geq 10^8$ cfu/ml) during the first 3 dai, which corresponds to the differences in symptom development. The ΦPSII value was decreased at low inoculation concentrations ($\leq 10^4$ cfu/ml), which showed no visible symptoms. Infection of *Arabidopsis* by virulent and avirulent strains of Pst DC3000 led to a localized decline in F_v/F_m, ΦPSII, and NPQ before symptoms were visible to the naked eye (Bonfig et al., 2006). In addition, the changes occurred earlier and to a greater extent in leaves inoculated with the avirulent strain than

in leaves inoculated with the virulent strain, and they were also dependent on inoculum density. In bean leaves inoculated with low-dose (10^4 cfu/ml) *P. s*. pv. *phaseolicola*, there was no significant impact on F_v/F_m or ΦPSII (Rodríguez-Moreno et al., 2008). Therefore, the decrease in F_v/F_m and ΦPSII by inoculation of high concentrations ($\geq 10^6$ cfu/ml) indicate that *P. cichorii* may directly paralyze the PSII reaction centers.

There was only a slight reduction of NPQ in bean leaves inoculated with low-dose (10^4 cfu/ml) *P. s*. pv. *phaseolicola* (Rodríguez-Moreno et al., 2008). In our study, changes in NPQ values were not correlated with inoculated cell concentrations or symptom development. NPQ values increased slightly at low inoculation concentrations, but significantly decreased because of heavy tissue damage at high concentrations. Pérez-Bueno et al. (2015) suggested an initial increase of NPQ followed by a decline by suppression of the thylakoid when bacterial concentrations reach a certain level. In this study, among the three parameters analyzed, we observed that ΦPSII maximized the difference between the inoculum densities.

Chlorophyll metabolism in the chloroplast, which is involved in regulation of defense signaling upon various stresses (Kangasjärvi et al., 2012), is reduced by pathogen infection. Pathogen infection causes collapse of chlorophyll. In this study, a reduction in chlorophyll content was observed 1 dai only when plants were inoculated with high inoculum densities ($\geq 10^6$ cfu/ml), and the decrease progressed until 3 dai. Since pathogens cause a reduction in leaf chlorophyll content due to necrotic or chlorotic lesions at later stages of infection, differentiation of extent and titer of inoculum concentrations was less informative than the chlorophyll fluorescence assay.

The detection of plant colonization by pathogens before the appearance of typical disease symptoms is crucial to controlling plant diseases. Recently, based on changes in plant physiology by pathogen infection, the development of imaging techniques, such as VIS/NIR and chlorophyll fluorescence hyperspectral and thermal imaging, facilitated the analysis of modulation in primary and secondary metabolism during biotic stresses (Belin et al., 2013; Pineda et al., 2011; Wagner et al., 2006). In this study, to select the wavelengths best suited for classifying infected leaves from healthy leaves and to visualize bacterial infection before symptom development, we inoculated various concentrations of *P. cichorii* into tomato plants and obtained VIS/NIR and chlorophyll fluorescence images. Among the VIS/NIR spectra from 400 to 1,000 nm, wavebands from 478 to 683 nm were selected using PCA-based statistical methods as the most effective for detecting pathogen infection. The VIS/NIR spectra in the infected areas shifted from yellow to red as necrosis progressed. Furthermore, the images identified non-symptomatic changes as well as pre-symptomatic changes, while physical damage was not clearly differentiated from pathogenic necrosis.

Delalieux et al. (2007) reported that hyperspectral spectra from 1,350 to 1,750 nm and 2,200 to 2,500 nm were effective for classification of *Venturia inaequalis*-infected leaves from healthy leaves in early disease stages, whereas wavelengths of 580–660 nm and 688–715 nm were effective for identifying infected leaves at more developed stages of infection. And among the statistical methods, logistic regression analysis, partial least squares logistic discriminant analysis, and tree-based modeling were preferred for classification. Purcell et al. (2009) obtained NIR spectroscopy and used PCA and PLS-based statistical methods to rate sugarcane resistance against Fiji leaf gall disease in sugarcane. In this study, chlorophyll fluorescence at 365 nm and 410 nm was effective in differentiating infected areas by shifting the spectra of the infected leaf areas to a blue color.

A detailed understanding of plant physiological processes related to specific diseases as well as detection and quantification of disease is indispensable. Overall, the results of this study demonstrate plant responses in photosynthesis depending on infection severity. Infection by *P. cichorii* led to changes in chlorophyll fluorescence parameters before visible symptoms were detectable, and infections that were not yet symptomatic also induced changes in the photosynthetic parameters. Our present results suggest that chlorophyll fluorescence measurements can be used as markers of infection. Furthermore, VIS/NIR and chlorophyll fluorescence hyperspectral image systems will provide information on the development of early detection techniques.

Acknowledgments

We gratefully acknowledge a grant from the Next-Generation BioGreen 21 Program (No. PJ01125603) of Rural Development Administration. This research was also supported in part by the Basic Science Research program (2014R1A1A4A01003957) through the National Research Foundation of Korea (NRF) funded by the Ministry of Education, Republic of Korea.

References

Belin, É., Rousseau. D., Boureau, T. and Caffier, V. 2013. Thermography versus chlorophyll fluorescence imaging for detection and quantification of apple scab. *Comput. Electron. Agric*. 90:159-163.

Berger, S., Papadopoulos, M., Schreiber, U., Kaiser, W. and

Roitsch T. 2004. Complex regulation of gene expression, photosynthesis and sugar levels by pathogen infection in tomato. *Physiol. Plant*. 122:419-428.

Berger, S., Sinha, A. K. and Roitsch, T. 2007. Plant physiology meets phytopathology: plant primary metabolism and plant-pathogen interactions. *J. Exp. Bot*. 58:4019-4026.

Bilgin, D. D., Zavala, J. A., Zhu, J., Clough, S. J., Ort, D. R. and DeLucia, E. H. 2010. Biotic stress globally downregulates photosynthesis genes. *Plant Cell Environ*. 33:1597-1613.

Bonfig, K. B., Schreiber, U., Gabler, A., Roitsch, T. and Berger, S. 2006. Infection with virulent and avirulent *P. syringae* strains differentially affects photosynthesis and sink metabolism in *Arabidopsis* leaves. *Planta* 225:1-12.

Chaerle, L., Hagenbeek, D., De Bruyne, E., Valcke, R. and Van Der Straeten, D. 2004. Thermal and chlorophyll-fluorescence imaging distinguish plant-pathogen interactions at an early stage. *Plant Cell Physiol*. 45:887-896.

Delalieux, S., Van Aardt, J., Keulemans, W., Schrevens, E. and Coppin, P. 2007. Detection of biotic stress (*Venturia inaequalis*) in apple trees using hyperspectral data: non-parametric statistical approaches and physiological implications. *Eur. J. Agron*. 27:130-143.

Dempsey, D. A. and Klessig, D. F. 2012. SOS: too many signals for systemic acquired resistance? *Trends Plant Sci*. 17:538-545.

Ehness, R., Ecker, M., Godt, D. E. and Roitsch, T. 1997. Glucose and stress independently regulate source and sink metabolism and defense mechanisms via signal transduction pathways involving protein phosphorylation. *Plant Cell* 9:1825-1841.

Farissi, M., Ghoulam, C. and Bouizgaren, A. 2013. Changes in water deficit saturation and photosynthetic pigments of alfalfa populations under salinity and assessment of proline role in salt tolerance. *Agric. Sci. Res. J*. 3:29-35.

Furbank, R. T. and Tester, M. 2011. Phenomics technologies to relieve the phenotyping bottleneck. *Trends Plant Sci*. 16:635-644.

Hung, N. B., Ramkumar, G. and Lee, Y. H. 2014. An effector gene *hopA1* influences on virulence, host specificity, and lifestyles of *Pseudomonas cichorii* JBC1. *Res. Microbiol*. 165:620-629.

Kangasjärvi, S., Neukermans, J., Li, S., Aro, E. M. and Noctor, G. 2012. Photosynthesis, photorespiration, and light signaling in defense responses. *J. Exp. Bot*. 63:1619-1636.

Kolber, Z., Klimov, D., Ananyev, G., Rascher, U., Berry, J. and Osmond, B. 2005. Measuring photosynthetic parameters at a distance: laser induced fluorescence transient (LIFT) method for remote measurements of photosynthesis in terrestrial vegetation. *Photosynth. Res*. 84:121-129.

Lee, W. H., Kim, M. S., Lee, H. S., Delwiche, S. R., Bae, H. H., Kim, D. Y. and Cho, B. K. 2014. Hyperspectral near-infrared imaging for the detection of physical damages of pear. *J. Food Eng*. 130:1-7.

Looseley, M. E. and Newton, A. C. 2014. Assessing the consequences of microbial infection in field trials: seen, unseen, beneficial, parasitic and pathogenic. *Agronomy* 4:302-321.

Murchie, E. H. and Lawson, T. 2013. Chlorophyll fluorescence analysis: a guide to good practice and understanding some new applications. *J. Exp. Bot*. 64:3983-3998.

Nagendran, R. and Lee, Y. H. 2015. Green and red light reduces the disease severity by *Pseudomonas cichorii* JBC1 in tomato plants via upregulation of defense-related gene expression. *Phytopathology* 105:412-418.

Pauwelyn, E., Vanhouteghem, K., Cottyn, B., De Vos, P., Maes, M., Bleyaert, P. and Höfte, M. 2011. Epidemiology of *Pseudomonas cichorii*, the cause of lettuce midrib rot. *J. Phytopathol*. 159:298-305.

Pérez-Bueno, M. L., Pineda, M., Díaz-Casado, E. and Barón, M. 2015. Spatial and temporal dynamics of primary and secondary metabolism in *Phaseolus vulgaris* challenged by *Pseudomonas syringae*. *Physiol. Plant.* 153:161-174.

Pineda, M., Olejníčková, J., Cséfalvay, L. and Barón, M. 2011. Tracking viral movement in plants by means of chlorophyll fluorescence imaging. *J. Plant Physiol*. 168:2035-2040.

Purcell, D. E., O'Shea, M. G., Johnson, R. A. and Kokot, S. 2009. Near-infrared spectroscopy for the prediction of disease ratings for Fiji leaf gall in sugarcane clones. *Appl. Spectrosc*. 63:450-457.

Refshauge, S. J., Nayudu, M., Vranjic, J. and Bock, C. H. 2010. Infection and dispersal processes of *Pseudomonas syringae* pv. *coriandricola* on coriander. *Phytopathol. Mediterr*. 49:42-50.

Rodríguez-Moreno, L., Pineda, M., Soukupová, J., Macho, A. P., Beuzón, C. R., Barón, M. and Ramos, C. 2008. Early detection of bean infection by *Pseudomonas syringae* in asymptomatic leaf areas using chlorophyll fluorescence imaging. *Photosynth. Res*. 96:27-35.

Rojas, C. M., Senthil-Kumar, M., Tzin, V. and Mysore, K. S. 2014. Regulation of primary plant metabolism during plant-pathogen interactions and its contribution to plant defense. *Front. Plant Sci*. 5:17.

Stromberg, K. D., Kinkel, L. L. and Leonard, K. J. 1999. Relationship between phyllosphere population sizes of *Xanthomonas translucens* pv. *translucens* and bacterial leaf streak severity on wheat seedlings. *Phytopathology* 89:131-135.

Tao, Y., Xie, Z., Chen, W., Glazebrook, J., Chang, H. S., Han, B., Zhu, T., Zou, G. and Katagiri, F. 2003. Quantitative nature of *Arabidopsis* responses during compatible and incompatible interactions with the bacterial pathogen *Pseudomonas syringae*. *Plant Cell* 15:317-330.

Uppalapati, S. R., Ishiga, Y., Wangdi, T., Urbanczyk-Wochniak, E., Ishiga, T., Mysore, K. S. and Bender, C. L. 2008. Pathogenicity of *Pseudomonas syringae* pv. *tomato* on tomato seedlings: phenotypic and gene expression analyses of the virulence function of coronatine. *Mol. Plant-Microbe Interact*. 21:383-395.

Wagner, A., Michalek, W. and Jamiokowska, A. 2006. Chlorophyll fluorescence measurements as indicators of fusariosis severity in tomato plants. *Agron. Res*. 4:461-464.

Wang, M., Xiong, Y., Ling, N., Feng, X., Zhong, Z., Shen, Q. and Guo, S. 2013. Detection of the dynamic response of cucumber leaves to fusaric acid using thermal imaging. *Plant Physiol. Biochem*. 66:68-76.

Yu, S. M. and Lee, Y. H. 2012. First report of *Pseudomonas cichorii* associated with leaf spot on soybean in South Korea. *Plant Dis*. 96:142.

Zou, J., Rodriguez-Zas, S., Aldea, M., Li, M., Zhu, J., Gonzalez, D. O., Vodkin, L. O., DeLucia, E. and Clough, S. J. 2005. Expression profiling soybean response to *Pseudomonas syringae* reveals new defense-related genes and rapid HR-specific downregulation of photosynthesis. *Mol. Plant-Microbe Interact*. 18:1161-1174.